Supporting Information

Experimental Details

An electrolyte-supported planar-type single cell 17 mm in diameter and 0.3 mm in thickness was used, and $La_{0.9}Sr_{0.1}Ga_{0.8}Mg_{0.2}O_3$ (LSGM) was prepared by a conventional solid-solution method using La_2O_3, $SrCO_3$, Ga_2O_3, and MgO as starting materials. The mixed powder was calcined at 1273 K for 6 h before being pressed into a disk and sintered at 1773 K for 6 h. The LSGM disk was polished to a thickness of 0.3 mm. **Figure S1** shows the XRD patterns of LSGM electrolyte before and after measurement.   It is evident that all diffraction peaks were assigned to those from $LaGaO_3$ phase suggesting no impurity phase.   It is also noted that no significant difference were observed after measurement suggesting that stability of LSGM electrolyte is also reasonably high.

Ni–Fe (Ni:Fe = 9:1, molar ratio) used as the anode was synthesized by loading $Fe(NO_3)_3 \cdot 9H_2O$ of NiO in an aqueous solution. The obtained powder was calcined in air at 873 K for the decomposition of nitrate acid. $Sm_{0.5}Sr_{0.5}CoO_3$ (SSC) cathode was prepared by the solid-state reaction method. $NiO–Fe_2O_3$ and SSC powders were painted on each face of the LSGM disk to 5 mm in thickness by a screen printing method followed by calcination at 1373 K for 30 min. The prepared planar-type single cell was set in an Al_2O_3 tube with molten Pyrex glass used as a gas sealant. Fe oxide (ca. 0.1 g) was fixed under the planar-type SOFC with quartz wool. After heating the cell, humidified hydrogen (3 vol% H_2O) was first fed into the Fe room to reduce the Ni–Fe anode and Fe powder to metallic states. After reduction, the Fe room was separated by two stop valves from a gas supply line. The discharge capacity of the cell was measured by the four-probe method under the application of the constant current of 50 mA/cm^2, or that otherwise noted.   Since the capacity of 40 mAh was always observed at potential higher than 0.95V without Fe oxide in the anode side room, the observed capacity was always subtracted by 40 mAh for estimating the capacity of Fe oxidation.

For charging process, electrochemical pumping of oxygen forms H_2 by electrolysis of humidity resulting in reducing Fe oxide to Fe, however, it takes longer period.   Therefore, in this study, we used H_2 flow for reducing Fe oxide to Fe instead of electrochemical pumping of oxygen.
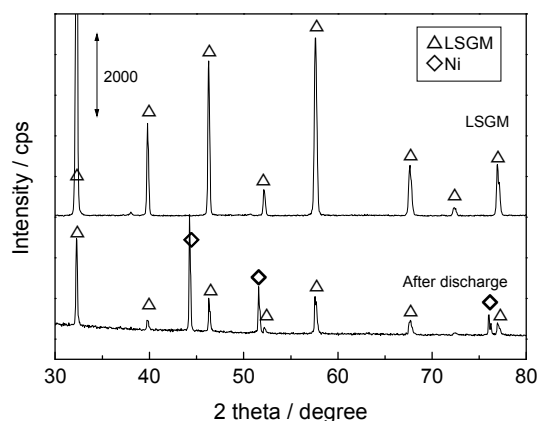
Figure S1   XRD patterns of LSGM electrolyte before and after measurement.

Chemical equilibrium of Fe oxide state.

Figure S2 shows the Fe oxide state at marked temperature as a function of oxygen partial pressure so-called "Keringum diagram".   Evidently, with decreasing temperature, oxygen partial pressure of Fe oxide with higher oxidation number becomes wider and so lower operation temperature of the cell has an advantage of larger theoretical capacity. It is also noted that at temperature lower than 873 K, 10^{-20} atm, the most stable phase of Fe oxide is Fe_2O_3.   Therefore, at room temperature, the most stable state of Fe is Fe_2O_3, and at 873 K, $P_{O2}=10^{-18}$ atm, Fe_3O_4 is the most stable oxidation state.
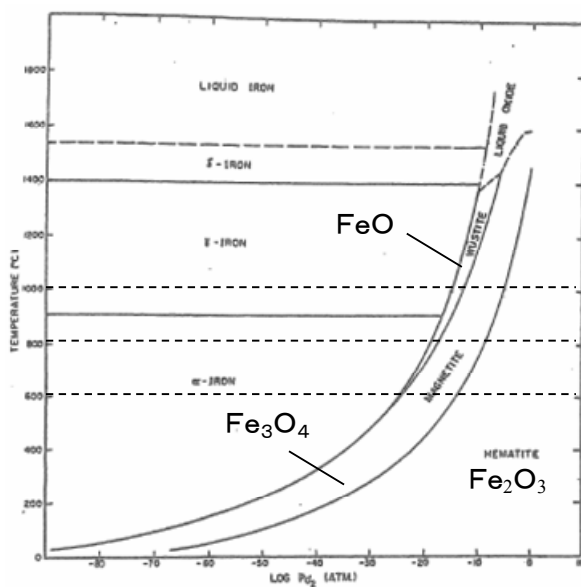

Figure S2   Keringum diagram of Fe.